1 **Cloud scavenging of abundant anthropogenic refractory particles at a**

2 **mountain site in North China**

3 Lei Liu[1,2], Jian Zhang[1,2], Liang Xu[1,2], Qi Yuan[2], Dao Huang[2], Jianmin Chen[3], Zongbo Shi[4], Yele Sun[5],

4 Pingqing Fu[5], Zifa Wang[5], Daizhou Zhang[6], Weijun Li[2,*]

5

6 [1]Environment Research Institute, Shandong University, Jinan 250100, China

7 [2]Department of Atmospheric Sciences, School of Earth Sciences, Zhejiang University, Hangzhou 320007, China

8 [3]Shanghai Key Laboratory of Atmospheric Particle Pollution and Prevention, Department of Environmental Science

9 and Engineering, Fudan University, Shanghai 200433, China

10 [4]School of Geography, Earth and Environmental Sciences, University of Birmingham, Birmingham B15 2TT, UK

11 [5]State Key Laboratory of Atmospheric Boundary Layer Physics and Atmospheric Chemistry, Institute of Atmospheric

12 Physics, Chinese Academy of Sciences, Beijing 100029, China

13 [6]Faculty of Environmental and Symbiotic Sciences, Prefectural University of Kumamoto, Kumamoto 862-8502, Japan

14 *Correspondence to*: Weijun Li (liweijun@zju.edu.cn)

Atmospheric
Chemistry
and Physics
Discussions

15   **Abstract.** Aerosol-cloud interaction remains a major source of uncertainty in climate forcing estimate.

16   Our knowledge about the aerosol-cloud interaction is particularly weak in heavily polluted conditions.

17   In this study, cloud residual (cloud RES) and cloud interstitial (cloud INT) particles were collected

18   during cloud events under different pollution levels from 22 July to 1 August, 2014 at Mt. Tai (1532 m

19   above sea level) located in the North China Plain (NCP). Transmission electron microscopy (TEM) was

20   used to investigate size, composition, and mixing state of individual cloud RES and INT particles. Our

21   results show that S-rich particles were predominant (78%) during clean periods ($PM_{2.5} < 15$ µg m^{-3}), but

22   a large amount of anthropogenic refractory particles (e.g., soot, fly ash, and metal) and their mixture

23   with S-rich particles (named as S-refractory) were observed during polluted periods. Cloud droplets

24   collected during polluted periods were found to become an extremely complicated mixture by

25   scavenging of abundant refractory particles. We found that 76% of cloud RES were S-refractory

26   particles and that 26% of cloud RES contained two or more types of refractory particles.

27   Soot-containing particles (i.e., S-soot and S-fly ash/metal-soot) were the most abundant (62%) among

28   cloud RES, followed by fly ash/metal-containing particles (i.e., S-fly ash/metal and S-fly ash/metal-soot,

29   37%). The complicated cloud droplets have not been reported in clean continental or marine air before.

30   Our findings provide an insight into the potential impacts on cloud radiative forcing from black carbon,

31   atmospheric biogeochemical cycle and metal catalysis reactions of SO_2 in micro-cloud droplets from

32   soluble metals releasing from fly ash and metals in cloud droplets over polluted air.

Atmospheric
Chemistry
and Physics
Discussions

1. Introduction

33

34   Clouds play a crucial role in various physical and chemical processes occurring in the lower

35   troposphere and hence affect the Earth's radiation budget (Seinfeld et al., 2016;Tilgner et al., 2014).

36   Aerosol particles, including primary and secondary ones generated from natural and anthropogenic

37   sources, either directly alter radiative forcing or act as cloud condensation nuclei (CCN) to indirectly

38   influence it. At present, aerosol-cloud interactions unquestionably affect radiative forcing and global

39   climate (McFiggans et al., 2006;Seinfeld and Pandis, 2006;Rosenfeld et al., 2014). CCN become cloud

40   droplets through the condensation of water vapor when the relative humidity (RH) of an air parcel

41   increases above saturation (Farmer et al., 2015). Size, chemical composition, and mixing state are main

42   factors affecting the ability of a particle to act as CCN (Dusek et al., 2006;Li et al., 2011a;Fan et al.,

43   2016;Rosenfeld, 2000;Hudson, 2007). In addition, aerosol particles incorporated into cloud droplets can

44   be easily lifted into the free troposphere during cloud development and further extend their influence on

45   cloud precipitation and regional climate (Fan et al., 2016).

46   Owing to the rapid industrialization and urbanization in Asia, large quantities of aerosol particles

47   from anthropogenic sources are released into the atmosphere, which can dramatically affect the

48   chemical composition of clouds (Li et al., 2011b;Drewnick et al., 2007;Ervens, 2015;Twohy and

49   Anderson, 2008). High concentrations of aerosol particles increase the number of cloud droplets and

50   reduce their size, which further results in the reduction of precipitation efficiency and in extending the

51   lifetime of clouds (McFiggans et al., 2006;Qian et al., 2009;Fan et al., 2016;Li et al., 2017a;Rosenfeld,

52   2000). Moreover, anthropogenic aerosol particles - especially fly ash, metal, and soot particles - are

53   incorporated into cloud droplets, and be transported long distances to affect ecosystems, human health,

54   and radiative forcing (Li et al., 2013;Rosenfeld et al., 2014). Especially the toxic and bioaccumulative

55   metals can deposit into the ecosystem following fog or precipitation and further cause severe health

56   problems to human beings (Liu et al., 2012). Moreover, transition metals such as iron (Fe) and

57   manganese (Mn) can enhance the in-cloud oxidation of sulfur dioxide to sulfate (Harris et al., 2013). It

58   is noteworthy that the Fe-bearing particles (e.g., fly ash and metal) emitted from industrial activities can

59   be beneficial to remote ocean ecosystems (Li et al., 2017b).

60   Recently, many studies have been performed worldwide to investigate aerosol-cloud interactions

61   and the composition of cloud droplets. Schroder et al. (2015) investigated the activation of refractory

Atmospheric
Chemistry
and Physics
Discussions

62   black carbon (BC) particles in stratocumulus clouds at a marine boundary layer site using a counterflow

63   virtual impactor and single particle soot photometer. Ueda et al. (2014) reported the effects of in-cloud

64   processes on the compositional changes of sea salt particles by collecting individual aerosol particles in

65   and below clouds, respectively. Pierce et al. (2015) calculated size distribution changes and radiative

66   forcing effects due to the scavenging of interstitial particles by cloud droplets in a clean, remote region.

67   Roth et al. (2016) analyzed the composition and mixing state of cloud residues and out-of-cloud aerosol

68   particles by single particle aerosol mass spectrometry on a mountain site and found that soot particles

69   internally mixed with sulfate and nitrate were the dominant ones in cloud residues. All of the above

70   studies were carried out in clean atmosphere, they could not observe the clear interactions between

71   abundant anthropogenic particles and cloud droplets. However, the latest satellite observations indicated

72   that large amounts of anthropogenic fine particles assembled in cloud base and might modify cloud

73   properties in heavily polluted air influenced by industrial and urban emissions (Eck et al., 2018). Field

74   observations are requested to confirm it and understand the interactions of aerosol-cloud over polluted

75   areas, especially in North and South Asia.

76   Mt. Tai, the highest mountain in the NCP, is surrounded by several medium-sized industrial cities.

77   The altitude of Mt. Tai is close to the top of the planetary boundary layer (PBL) above the NCP.

78   Therefore, Mt. Tai is an ideal site to study the effects of regional transport and local emissions of

79   anthropogenic aerosols on cloud properties. Many studies have been conducted on Mt. Tai, but virtually

80   all the researchers mainly focus on the variation of chemical composition and size distribution of

81   aerosol particles (Zhang et al., 2014) and chemical compositions of cloud water (Li et al., 2017a;Wang

82   et al., 2011). Because of the limitation of sampling and analyzing techniques, these studies did not

83   consider the aerosol-cloud interactions at the top of Mt. Tai in North China.

84   Transmission electron microscopy (TEM) has become a powerful technique to characterize the

85   morphology, composition, size, and mixing state of individual aerosol particles in recent years (Li et al.,

86   2016a;Ueda et al., 2014). Many studies used single particle aerosol mass spectrometry (SPAMS) to

87   characterize the composition and mixing state of residual particles of individual cloud droplets (Zhang

88   et al., 2017;Lin et al., 2017;Pratt et al., 2010). Compared to the SPAMS, TEM can directly observe the

89   morphology and mixing state of individual cloud droplet residual (cloud RES) and interstitial particles

90   (cloud INT) (Ueda et al., 2014;Twohy and Anderson, 2008;Li et al., 2011a;Kojima et al., 2004).

91   Therefore, TEM technique can not only be used to identify cloud RES and cloud INT collected in a

Atmospheric
Chemistry
and Physics
Discussions

92 same cloud event but also capture interactions between aerosol-clouds based on mixing state of

93 individual particles. In this study, we collected individual particles during cloud events at the summit of

94 Mt. Tai and applied TEM to obtain and compare the size, morphology, composition, and mixing state of

95 cloud RES and cloud INT. This is helpful to understand the influence of anthropogenic sources on cloud

96 properties above the heavily polluted region.

97 2. Experimental methods

98 2.1 Sampling sites

99 Field observations were carried out at Mt. Tai (36.251°N, 117.101°E; 1532 m above sea level (a.s.l))

100 from 22 July to 1 August 2014. Mt. Tai is the highest mountain in the central NCP and is surrounded by

101 many medium-sized industrial cities (Fig. 1). Many coal-fired power plants, oil refinery plants, steel

102 plants, and cement plants are located in these industrial cities (Jinan, Zibo, Laiwu, Liaocheng, Jining,

103 Tai'an etc.) within a radius of 120 km around Mt. Tai (Fig. 1b). Jinan city is the capital of Shandong

104 Province and is situated 60 km north of Mt. Tai. Tai'an city is located at the southern foot of Mt. Tai.

105 Therefore, the local and regional emissions may have a large contribution to the air quality at the

106 summit of Mt. Tai. Mt. Tai's altitude is close to the top of planetary boundary layer over the NCP, and

107 local cloud events frequently occur at its summit, especially in summer.

108 As shown in Fig. 1c, individual particle samples were collected at a sampling site near the summit

109 of Mt. Tai. The sampling site was usually covered by clouds when cloud events occurred during the

110 sampling periods. The 24-h air mass backward trajectories arriving at Mt. Tai at 1500 m above ground

111 level (a.g.l) (Fig. 1a) were calculated using the Hybrid Single-Particles Lagrangian Integrated Trajectory

112 (HYSPLIT) model available at the NOAA Air Resources Laboratory's web server (Draxler and Rolph,

113 2003).

Atmospheric
Chemistry
and Physics
Discussions

Open Access
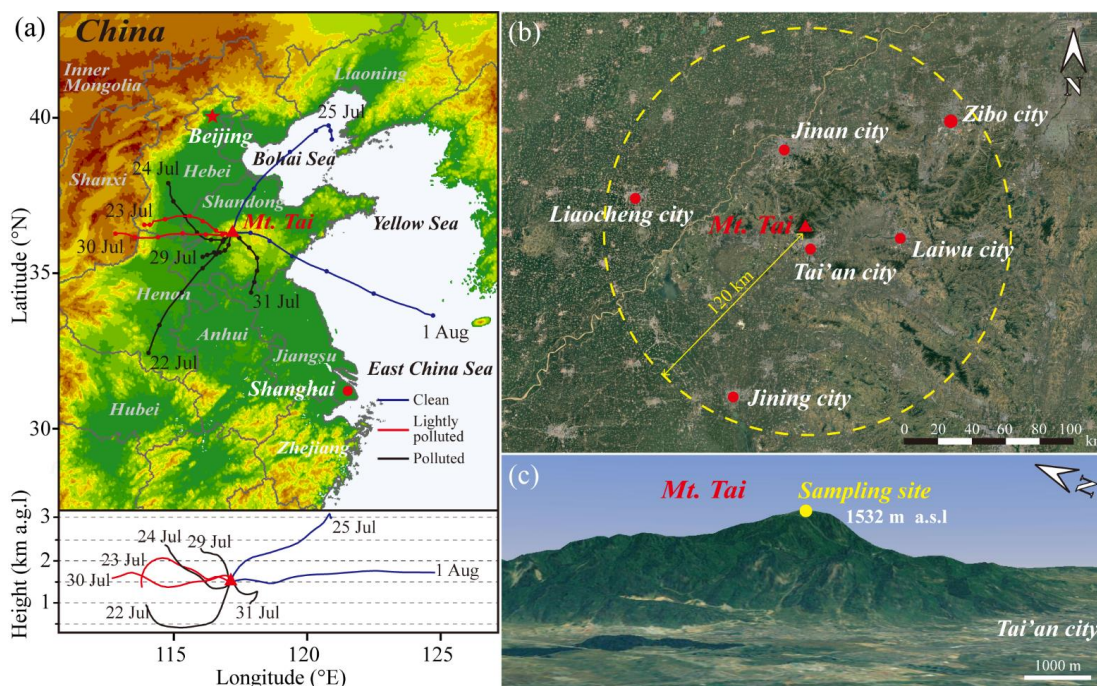
Figure 1. (a) Location of Mt. Tai in the North China Plain and the 24-h air mass backward trajectories arriving at Mt. Tai at 1500 m a.g.l during the sampling period. (b) The medium-sized industrial cities distributed within a radius of 120 km around Mt. Tai. (c) The expanded topographic view of Mt. Tai and the sampling site near the summit of Mt. Tai.

2.2 Individual particle collections

Individual aerosol particles were collected onto carbon films supported by TEM copper grids (carbon type-B, 300-mesh copper, Tianld Co., China) using a single-stage cascade impactor with a 0.5 mm diameter jet nozzle at a flow rate of 1.0 L min^{-1}. The aerodynamic diameter of particles collected with a 50% efficiency (cutoff diameter, d_{50}) by this individual sampler is 0.24 μm if particle density is 2 g cm^{-3}. More detailed information about the setup of a modified sampler can be found in our previous paper (Li et al., 2011a). The sample information in the present study is listed in Table 1.

During the sampling period, meteorological data at the summit of Mt. Tai including pressure (P), relative humidity (RH), temperature (T), wind speed (WS), and wind direction (WD) were measured and recorded every 5 min by a pocket weather meter (Kestrel 4500, Nielsen-Kellermann Inc., USA). PM$_{2.5}$ concentrations on Mt. Tai were monitored on-line by a beta attenuation and optical analyzer (model 5030 SHARP monitor, Thermo Scientific, USA).

Atmospheric
Chemistry
and Physics
Discussions

131   **Table 1.** Information on individual particle samples collected on Mt. Tai.

Sample ID	Sampling time (local time)	PM$_{2.5}$ ($\mu g\ m^{-3}$)	T (°C)	RH (%)	P (hPa)	WS (m s^{-1})
1	22 Jul. 2014 16:04	51.6	22.8	100	849.1	0.9
2	23 Jul. 2014 08:00	24.2	20.4	100	849.4	2.5
3	24 Jul. 2014 07:43	74.3	19.2	100	848.0	0
4	25 Jul. 2014 17:00	11.8	13.9	100	838.0	5.5
5	29 Jul. 2014 16:18	72.9	20.8	95.7	848.0	1.1
6	30 Jul. 2014 19:24	24.2	17.5	100	844.2	0.8
7	31 Jul. 2014 17:30	56.4	18.1	100	849.0	0.9
8	01 Aug. 2014 17:56	14.7	18.8	100	849.1	1.8

132   **2.3 TEM analysis**

133   Individual aerosol particles collected on TEM grids were analyzed by a transmission electron

134   microscope (TEM, JEM-2100, JEOL Ltd., Japan) at a 200 kV accelerating voltage. TEM is equipped

135   with an energy-dispersive X-ray spectrometer (EDS, INCA X-Max^N 80T, Oxford Instruments, UK).

136   EDS semi-quantitatively detects the elemental composition of individual particles with atomic number

137   greater than six ($Z > 6$). However, Cu peaks in the EDS spectra were not considered because of the

138   interference from the copper substrate of TEM grids. We acquired morphology, composition, and

139   mixing state of individual particles through the combination of TEM and EDS (TEM/EDS).

140   The distribution of aerosol particles on TEM grids was not uniform, with particle size decreasing

141   from the center to the edge of the TEM grids. The cloud droplets with larger size normally impacted on

142   the center and interstitial particles distributed the peripheral areas of TEM grids (Li et al., 2011a).

143   Moreover, the cloud RES had large rims compared with cloud INT, suggesting that the cloud RES were

144   droplets before being captured (Zhang et al., 2006). According to the distribution and morphology of

145   individual particles on the substrate, we can separate cloud RES and cloud INT particles. Figure 2

146   generally displays typical TEM images of cloud RES and cloud INT particles. In a word, many previous

147   studies using the cascade impactor have successfully captured individual interstitial particles and cloud

148   droplets on the substrate during cloud events (Ueda et al., 2014;Zhang et al., 2006;Kojima et al.,

149   2004;Li et al., 2011a).

150   To obtain the size of cloud RES and cloud INT particles, we measured the area and equivalent

151   circle diameter (ECD) of these analyzed particles by iTEM software (Olympus soft imaging solutions

152   GmbH, Germany). It should be noted that we measured ECD of the core of individual cloud RES

153   excluding the water rim because water rim only contains trace organics (Li et al., 2011a). The ECD can

154   be further converted to equivalent spherical diameter (ESD) according to the AFM analysis (see the

155   Supplement).
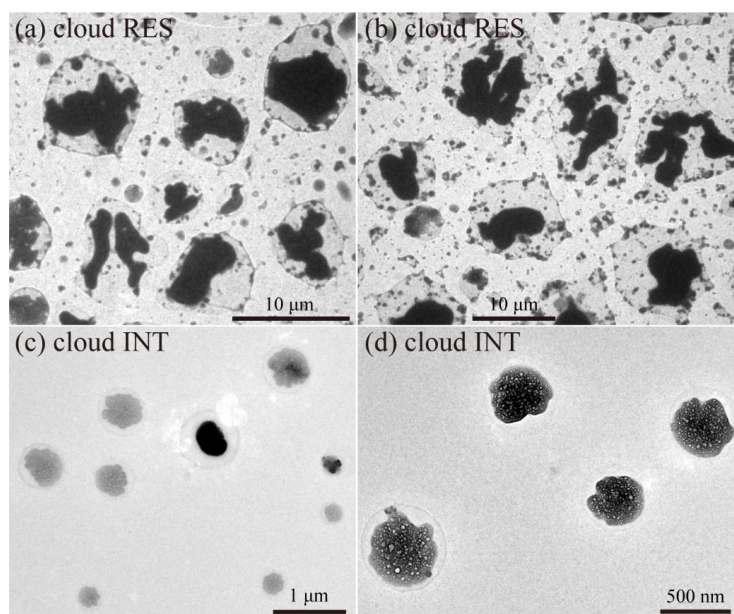
156

157   **Figure 2**. Low magnification TEM images of cloud RES (a-b) and cloud INT (c-d) particles collected

158   on Mt. Tai.

Atmospheric
Chemistry
and Physics
Discussions

Open Access

EGU

3. Results

3.1 Meteorological conditions and backward trajectories

Temporal variations of pressure (P), relative humidity (RH), temperature (T), wind speed (WS), wind direction (WD), and $PM_{2.5}$ concentration were measured on Mt. Tai from 22 July to 2 August 2014 (Fig. 3). During the sampling period, the temperature ranged from 12.6 to 29.4 $^{\circ}$C, and the RH varied between 48.2% and 100%. Each day during the sampling period, the RH reached 100% as temperatures decreased from the late afternoon into the evening (Fig. 3). We noticed that $PM_{2.5}$ concentrations on the mountaintop were closely related to wind direction and speed during the regional transport of hazes. Based on backward trajectories of air masses and $PM_{2.5}$ concentrations, the whole sampling period can be divided into three categories: *clean period* ($PM_{2.5} < 15$ μg m^{-3}), the prevailing winds were from the northeast to east and air masses were from higher altitudes above the marine areas which lead to the lowest $PM_{2.5}$ concentration; *lightly polluted period* (15 μg m$^{-3} < PM_{2.5} < 35$ μg m^{-3}), the prevailing winds were from the west, and air masses originating from higher altitudes above continental areas brought regional pollutants to the summit of Mt. Tai; *polluted period* ($PM_{2.5} > 35$ μg m^{-3}), air masses originating from northwest, southwest, or south went through Tai'an city. Back trajectories as shown in Fig. 1a during polluted days suggest that air pollutants from industrialized cities might be lifted along the southern slope up to Mt. Tai's summit.

Atmospheric
Chemistry
and Physics
Discussions
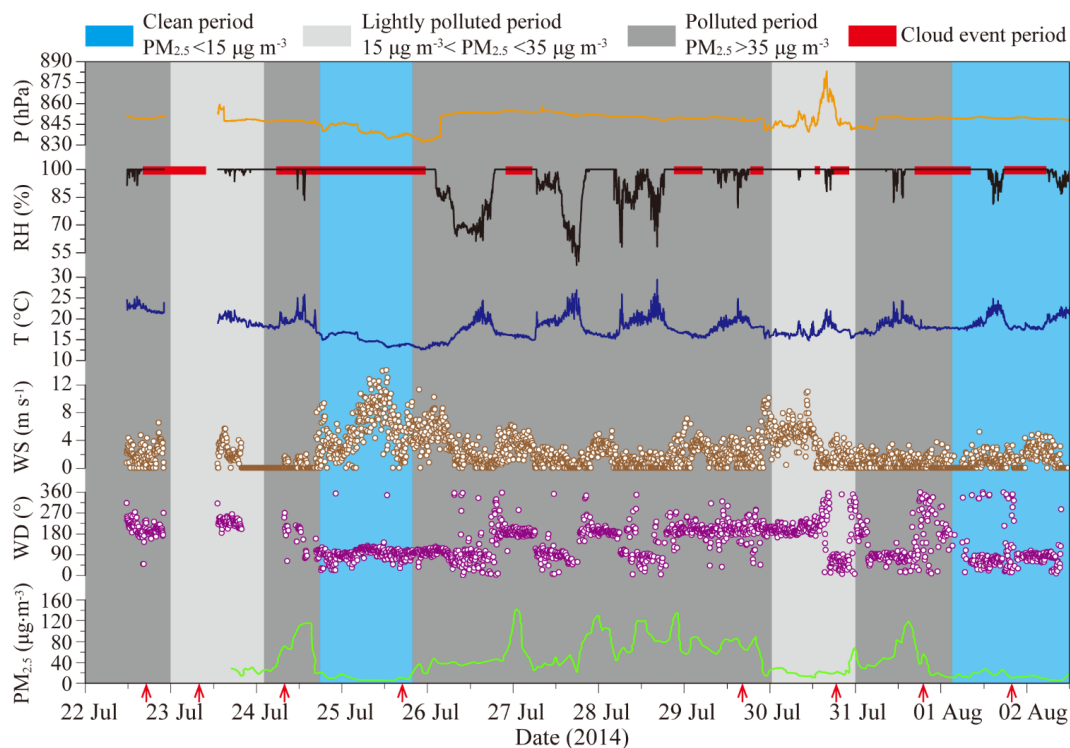
Figure 3. Temporal variations of pressure (P), relative humidity (RH), temperature (T), wind speed (WS), and wind direction (WD) measured on Mt. Tai from 22 July to 2 August 2014. The red arrows indicate collection times of individual particle samples during the cloud events.

Atmospheric
Chemistry
and Physics
Discussions

3.2 Mixing state of anthropogenic refractory particles

180

181   Based on their elemental composition and morphology, individual particles were classified into six

182   basic types: S-rich (Fig. S2a), soot (Fig. S2b), organic matter (OM, Fig. S2c), mineral (Fig. S2d), and

183   fly ash/metal (Figs. S2e-h). The classification criteria of different particle types and their sources have

184   been described in our previous study (Li et al., 2016a). S-rich particles representing secondary inorganic

185   particles (e.g., SO_4^{2-}, NO_3^-, and NH_4^+) are transformed from gaseous SO_2, NO_x, and NH_3. OM can be

186   divided into primary organic matter (POM) and secondary organic matter (SOM). POM is directly

187   emitted from coal or biomass burning and normally has spherical or irregular shapes (Liu et al., 2017),

188   whereas SOM is produced from the chemical oxidation of volatile organic compounds (VOCs) and

189   exhibits OM-coating on S-rich particles (Li et al., 2016b). Fly ash (e.g., Si, Al, and O) and metal

190   particles (e.g., Fe, Mn, Zn, and Pb) normally are emitted from coal-fired power plants and heavy

191   industrial activities, such as steel mills and smelters. Soot particles (i.e., BC) are generated from

192   incomplete combustion processes of biomass burning and fossil fuels in both industrial activities and

193   vehicular emissions. Mineral particles come from construction activities, resuspended road dust, and

194   natural soil. Among these types of particles, soot, POM, fly ash, mineral, and metal particles were

195   refractory under electron beams and were thus termed as refractory particles (Ebert et al., 2016).

196   Based on the mixing properties of individual particles (Figs. 4 and 5), they can be further classified

197   into four categories: S-mineral (Figs. 4a and 5a), S-soot (Figs. 4b and 5b), S-fly ash/metal (Figs. 4c and

198   5c), S-fly ash/metal-soot (Figs. 4d and 5d). Here, these four types of particles with refractory inclusions

199   are generally defined as "S-refractory" particles.

200
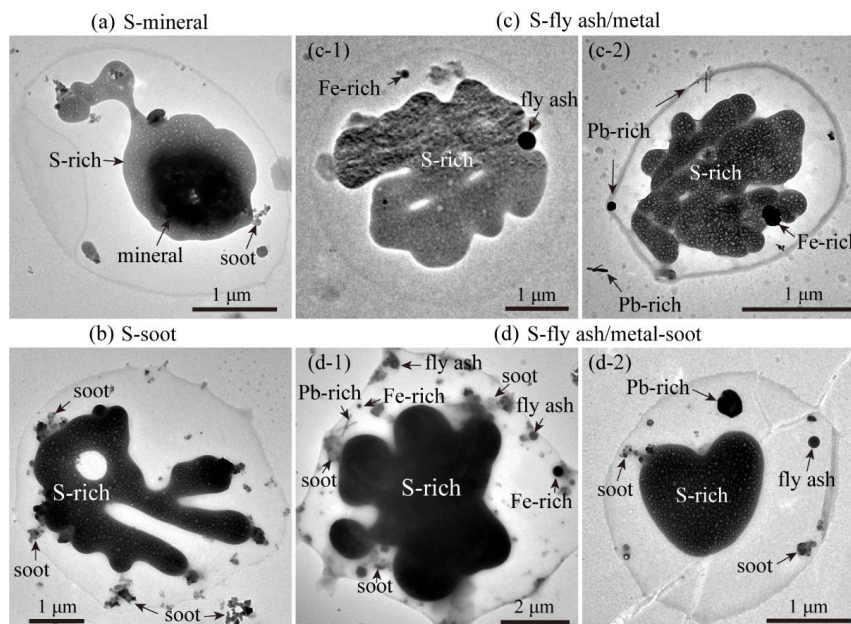
Figure 4. Typical TEM images of individual internally mixed cloud RES particles: (a) a mixture of

S-rich and mineral; (b) a mixture of S-rich and soot; (c) a mixture of S-rich and fly ash/metal; (d) a

mixture of S-rich, soot, and fly ash/metal.

204
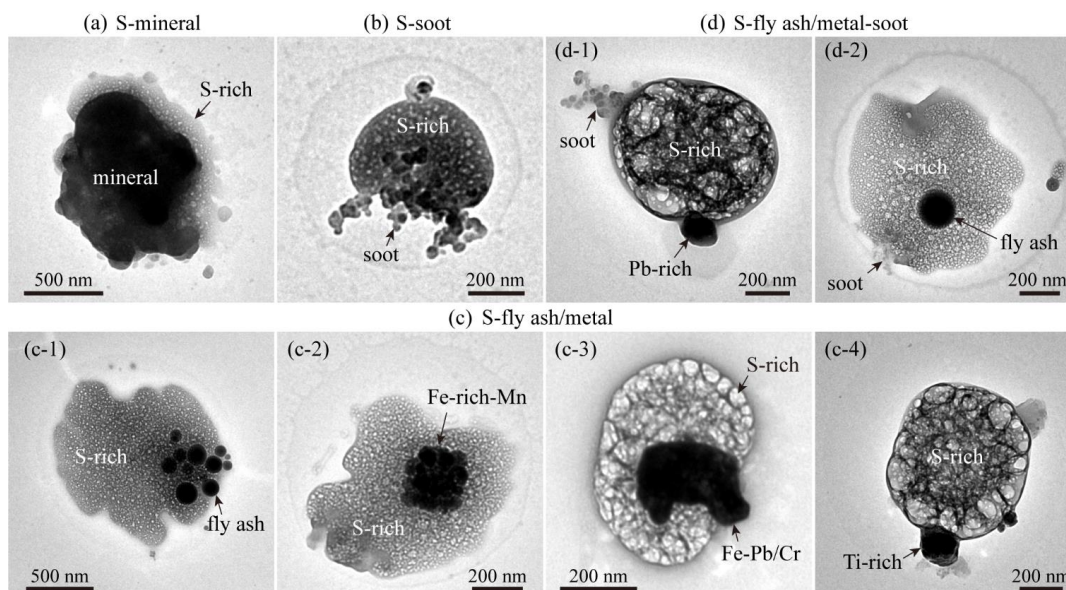
Figure 5. Typical TEM images of individual internally mixed cloud INT particles: (a) a mixture of

S-rich and mineral; (b) a mixture of S-rich and soot; (c) a mixture of S-rich and fly ash/metal; (d) a

mixture of S-rich, soot and fly ash/metal.

Atmospheric
Chemistry
and Physics
Discussions

208

209   Figure 6 shows number fractions of S-rich, refractory, and S-refractory particles in clean, lightly

210   polluted, and polluted periods on Mt. Tai. In clean periods, S-rich particles had the highest proportion

211   (78%), followed by a 22% contribution of the refractory and S-refractory particles. This may be

212   attributed to the clean air masses that originated from the clean marine area and arrived at the summit of

213   Mt. Tai through high-altitude transport (above 1500 m) (Fig. 1). Because the air masses did not contact

214   the ground surface, the local anthropogenic pollutants (e.g., soot, fly ash, and metal) could not be lifted

215   to the summit of Mt. Tai. Hence, secondary particles like S-rich were dominant in the clean period. In

216   the lightly polluted and polluted periods, the fraction of S-rich particles decreased to 59% and 44%,

217   respectively; meanwhile, the fractions of refractory and S-refractory increased up to 41% and 56%,

218   respectively (Fig. 6). The backward trajectories suggest that these air masses went through the most

219   heavily polluted areas before they arrived at the mountaintop (Fig. 1). Air masses on two polluted days

220   (e.g., 22 and 31 July) were lifted from ground level to the atmospheric boundary layer. Our study shows

221   that number fractions of refractory and S-refractory particles significantly increased from clean to

222   polluted periods (Fig. 6). This result shows that large amounts of primary refractory particles from

223   ground-level anthropogenic sources were lifted into the upper air and were further internally mixed with

224   S-rich particles.

225
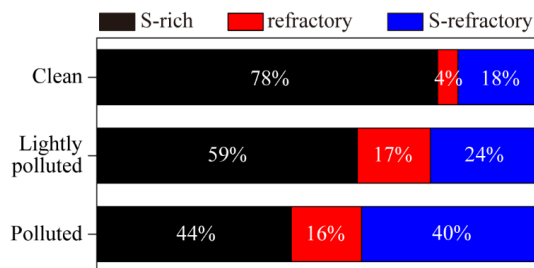
226   **Figure 6.** Number fractions of S-rich, refractory, and S-refractory particles at different pollution levels.

Atmospheric
Chemistry
and Physics
Discussions

3.4 Comparisons of cloud RES and INT particles

During the sampling period, a fog monitor was used to measure the size of cloud droplets during cloud events (Li et al., 2017a). This study reveals that in the cloud events all the cloud droplets displayed particle size larger than 2 μm in which size range the interstitial particles were absent. Based on their different sizes, we can know that these cloud droplets and interstitial particles impacted on different positions on the substrate. Although cloud droplets and interstitial particles became dry after the collection, we still can identify them based on the distribution and morphology of individual particles in TEM images (Li et al., 2011a;Ueda et al., 2014;Zhang et al., 2006;Kojima et al., 2004). Cloud RES display larger size and large rim around their CCN (Figs. 2 and 4) which has not been observed in non-cloud events. In contrast, cloud INT impacted on the position away from the center of sampling spot and their morphologies look like individual particles collected in non-cloud events. According to the rule, we can identify cloud RES and cloud INT in the samples collected during the cloud events.

Figure 7a shows that 100% of cloud RES and 83% of cloud INT contained S-rich species (i.e., S-rich and S-refractory). In other words, none of cloud RES were soot, fly ash/metal, and mineral particles but 17% of cloud INT were. Soot particles mainly distributed in the finer size bins (< 600 nm) of cloud INT (Fig. S3a). Interestingly, we found that 76% of cloud RES were a mixture of sulfates and refractory particles, 3.5 times higher than 22% in cloud INT (Fig. 7a). Furthermore, 26% of cloud RES had two or more types of inclusions (i.e., S-fly ash/metal-soot in Figs. 4d and 5d) but only 3% of cloud INT did. Therefore, we can conclude that cloud RES are an extremely complex mixture that forms when cloud droplets act like a collector to scavenge these refractory particles.

The size-resolved number fractions of different particle types in cloud RES and cloud INT indicate that S-rich particles were predominant from 60 nm to 1.2 μm in cloud INT (Fig. S3a), and S-refractory particles (indicated by the red box) dominated from 400 nm to 5.5 μm in cloud RES (Fig. S3b). Figure 7b shows that the median diameters of cloud RES and cloud INT were 1.19 μm and 422 nm, respectively. Sizes of cloud RES were much larger than that of cloud INT, suggesting that size is an important factor affecting the CCN ability (Dusek et al., 2006).

Atmospheric
Chemistry
and Physics
Discussions
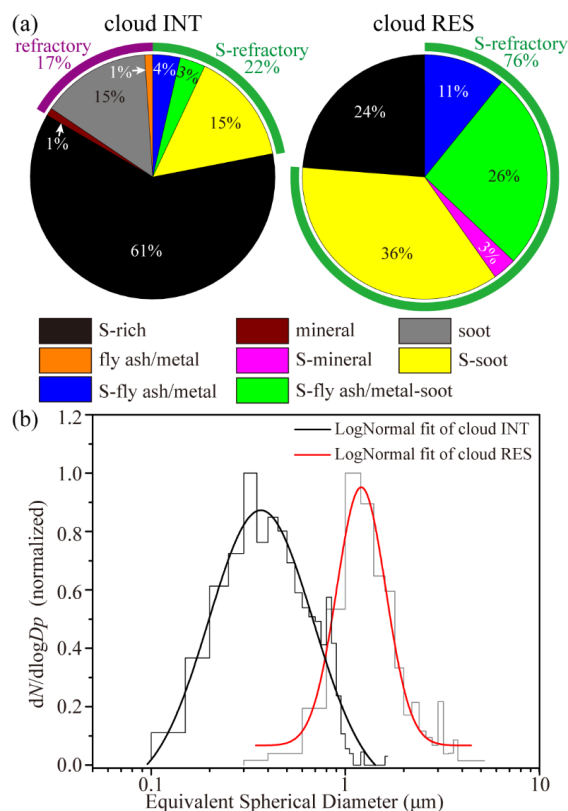
Figure 7. Number fractions of different particle types in cloud RES and INT particles (a) and size distributions of cloud RES and cloud INT particles (b). The measured particle sizes exclude the effects of water rims in TEM images. In total, 292 cloud RES and 1161 cloud INT particles were analyzed.

4. Discussion

TEM observations in this study reveals that cloud RES contained large amounts of refractory-containing particles primarily emitted from various anthropogenic sources in the heavily polluted NCP. As much as 76% of cloud RES were identified as S-refractory particles (Fig. 7a). We found that soot-containing particles (i.e., S-soot and S-fly ash/metal-soot) were the most abundant (62%) among the cloud RES, followed by the relatively abundant fly ash/metal-containing particles (i.e., S-fly ash/metal and S-fly ash/metal-soot, 37%) compared with 18% and 7% in the cloud INT, respectively (Fig. 7a). Although these refractory particles such as soot with hydrophobic properties could not be CCN directly, they can be easily accumulated by the existing cloud droplets as inclusions (Zuberi et al., 2005). In the heavily polluted NCP, large amounts of soot and fly ash/metal particles are released from anthropogenic sources (e.g., industrial activities and vehicular exhaust). During cloud events, abundant

269   refractory particles can be efficiently entrained into existing liquid cloud droplets by wet scavenging. Li

270   et al. (2011a) reported that the particle number decreased dramatically during cloud formation at Mt. Tai

271   with a scavenging ratio of 0.54, which demonstrated that aerosol particles could efficiently be

272   incorporated into cloud droplets. Physical coagulation of interstitial particles with cloud droplets is an

273   important process in developing clouds, which can lead to the reduction of cloud INT number and a size

274   increase of cloud RES after the cloud dries (Pierce et al., 2015). As we know so far, the extremely

275   complicated mixture of secondary and primary particles observed in the present study has seldom been

276   found in cloud droplets in clean air over developed countries (Ueda et al., 2014;Schneider et al.,

277   2017;Hao et al., 2013;Kojima et al., 2004), remote areas (Hiranuma et al., 2013), and ocean (Twohy and

278   Anderson, 2008;Hopkins et al., 2008;Zhang et al., 2006). For example, Zhang et al. (2006) reported that

279   S-rich particles were predominant in the cloud RES with a small number fraction of sea salt particles

280   over the Sea of Japan and soot or fly ash/metal particles were not observed. We believe that individual

281   cloud droplets are a far more complicated system in polluted air in North China than in the pristine

282   continental and clean ocean air of the world.

283   The cloud properties such as albedo and lifetimes could be largely modified by the aerosol-cloud

284   interactions, especially in heavily polluted regions (Wang et al., 2010;Wang et al., 2013). The model

285   simulation revealed that BC aerosols had a noticeable impact (up to nearly 20%) on cloud droplet

286   number concentration in polluted BC source regions (Cherian et al., 2017). Especially, abundant BC

287   particles incorporated into cloud droplets could lead to a decrease in cloud albedo by absorbing

288   radiation and an increase of temperature in troposphere, then accelerate the evaporation of the cloud

289   droplets (Zuberi et al., 2005;Ackerman et al., 2000;Adachi et al., 2010;Wang et al., 2013). In the past

290   few decades, precipitation was significantly reduced over east-central China due to the large amounts of

291   anthropogenic aerosols (Zhao et al., 2006;Qian et al., 2009). Because an excess of aerosols in clouds

292   could reduce precipitation, the non-precipitating clouds in the NCP tend to evaporate back to aerosol

293   particles by solar radiation. We believe that abundant BC particles presenting in the cloud droplets in the

294   heavily polluted NCP in this study (e.g., particle 1 and 2 in Fig. 8) significantly affected the cloud

295   properties and regional climate.

296   Fly ash and metal particles are a typical "fingerprint" pointing to the coal-fired power plants and

297   boilers in factories and heavy industries (e.g., steel plant and smelting factory) (Chen et al., 2012;Moffet

298   et al., 2008;Li et al., 2016a). Indeed, the most intense emissions from various industries in the world

299   occur in Hebei and Shandong provinces in the NCP (Qi et al., 2017). It is well known that these

300   industrial activities continuously release anthropogenic pollutants via high stacks into the upper air. Liu

301   et al. (2012) reported that the concentration of Zn reached 249.1 μg L^{-1} in the cloud/fog water samples

302   at Mt. Tai, followed by Al (157.3 μg L^{-1}), Fe (105.8 μg L^{-1}), Pb (46.2 μg L^{-1}), and Mn (42.8 μg L^{-1}),

303   which were extremely higher than those values reported at Mt. Schmücke in Germany (Fomba et al.,

304   2015). Combining these results with our present study, we infer that fine primary particles emitted from

305   these industrial activities might spread and be lifted to the upper air more easily than at ground level.

306   These metal particles, especially Pb and Zn of nanometer size, can harm ecosystems and human health

307   (Roberts et al., 2004). The fly ash and metal particles incorporated into cloud droplets (e.g., particle 1 in

308   Fig. 8) could go through the atmospheric acid Fe dissolution processes during long-range transport

309   reported by Li et al. (2017b). If they are further transported to remote oceanic regions, soluble Fe

310   species in the aerosol particles can fertilize plankton on the surface of ocean (Li et al., 2017b;Ito and Shi,

311   2016). Therefore, these anthropogenic fly ash/metal particles in polluted air contaminate cloud droplets

312   and further amplify potential impacts of fine metal particles on the biogeochemical cycle in the

313   troposphere.

314   Some studies suggested that the aqueous oxidation of SO_2 to sulfate by H_2O_2 and O_3 in cloud

315   droplets was dominant at Mt. Tai (Shen et al., 2012). However, cloud water collected on Mt. Tai

316   contained high concentrations of soluble Fe, Mn, Zn, and Pb (Liu et al., 2012). These soluble metals in

317   cloud droplets are released from aqueous reactions between metal particles and acidic sulfates in cloud

318   droplets (Li et al., 2017b). Harris et al. (2013) estimated that the oxidation of SO_2 in cloud droplets

319   catalyzed by natural transition metal ions (TMIs) in mineral dust was dominant at Mt. Schmücke in

320   Germany. For this study, how the soluble anthropogenic TMIs drive sulfate formation through TMI

321   catalysis in micro-cloud droplets is still a mystery in polluted air. We propose that anthropogenic TMI

322   catalysis contributing to sulfate production should be further considered in cloud droplets in the polluted

323   NCP.

324
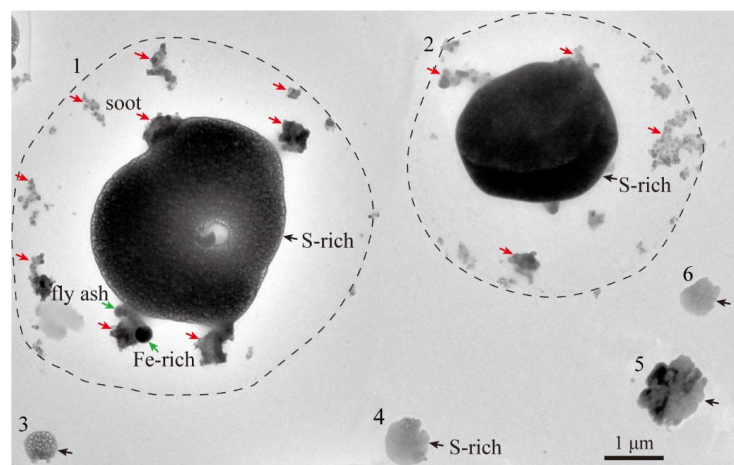
Figure 8. TEM image of cloud RES and INT particles collected during the cloud event occurred on the

polluted day of 31 July. Particle 1 and 2 are cloud RES and particle 3, 4, 5, and 6 are cloud INT. The

dashed lines indicate the water rims that were left after the cloud droplets impacting on the substrate

become dry.

The non-precipitating cloud processes over the polluted air of NCP quickly change the mixing states

and compositions of aerosol and cloud droplets in the upper air, potentially causing various effects such

as human health, regional climate, and biogeochemical cycle at the larger regional scale. To better

understand the aerosol-cloud interactions in this study, we offer the conceptual model of Fig. 9. The tall

stacks of plants can emit smoke plumes that contain fine refractory particles and gaseous pollutants to

the upper air. A portion of particles in urban areas can also be lifted to the mountaintop by prevailing

valley winds. Once the clouds form on a mountaintop (or later are transported in other directions), these

cloud droplets act as collectors to scavenge the refractory particles. These refractory particles as

inclusions might complicate the cloud chemistry in micro-cloud droplets. Gaseous pollutants such as

SO_2, NO_x, and VOCs may have enhanced aqueous oxidation potential in the complex cloud droplets.

Our study is designed to better understand the aerosol-cloud interactions on the mountaintop in polluted

industrial and urban areas. Recently, a study showed that the major aerosol pollution events with very

high fine mode AOD (>1.0 in mid-visible) in the China-Korea-Japan region are often observed to be

associated with significant cloud cover (Eck et al., 2018). Therefore, we expect that large amounts of

fine refractory particles from polluted areas scavenging in clouds have important impacts not only at

345   local but also in large regional scale.
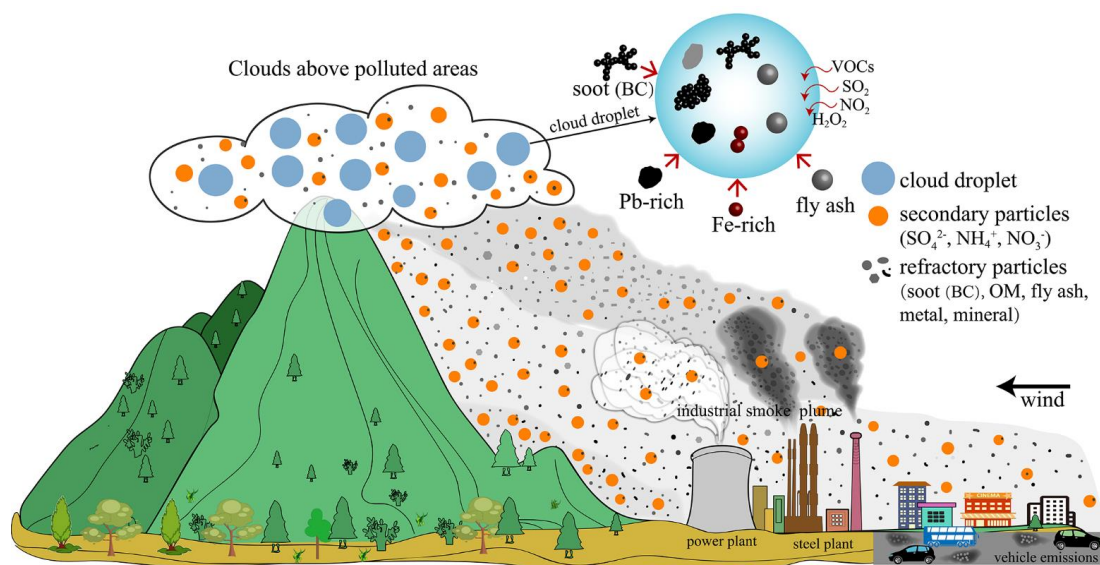
Figure 9. A conceptual model illustrating mechanisms of aerosol-cloud interactions on mountaintop influenced by anthropogenic pollutants from the heavy industrial and urban emissions.

5. Conclusions

Individual aerosol particles were collected during cloud events on Mt. Tai from 22 July to 1 August, 2014. Cloud RES and INT particles were separated by their distribution on TEM grids and their composition was identified by TEM/EDS. Individual particles were classified into S-rich, refractory (i.e., mineral, soot, fly ash/metal) and S-refractory (i.e., S-mineral, S-soot, S-fly ash/metal, and S-fly ash/metal-soot). According to air mass backward trajectories and $PM_{2.5}$ concentrations on Mt. Tai, the entire sampling period was divided into three classes: a clean period ($PM_{2.5} < 15$ μg m^{-3}), a lightly polluted period (15 μg m$^{-3} < PM_{2.5} < 35$ μg m^{-3}), and a polluted period ($PM_{2.5} > 35$ μg m^{-3}). In the clean period, individual particles were dominated by S-rich particles (78%), whereas the fraction of refractory particles and S-refractory particles increased significantly and dominated during the polluted periods. This suggested that anthropogenic pollutants from tall stacks of coal-fired power plants and heavy industries and vehicular exhaust in cities can be lifted to the summit of Mt. Tai under the prevailing southerly winds in summer.

TEM observations showed that 76% of cloud RES were S-refractory particles contaminated by anthropogenic refractory particles, compared with only 22% of cloud INT. Cloud RES displayed a

364   larger size than cloud INT, which indicates that particle size decidedly affects CCN ability. Our study

365   reveals that large amounts of anthropogenic refractory particles were incorporated into cloud droplets

366   through in-cloud processes. Especially important is that abundant BC particles in cloud droplets could

367   alter radiative forcing of clouds and accelerate the evaporation of cloud droplets. The high

368   concentrations of transition metal ions might favor the aqueous-phase oxidation of SO_2 by O_2 in cloud

369   droplets under the heavily polluted conditions in the NCP. Fly ash/metal-containing cloud droplets

370   could be transported long distances and harm ecosystems and human health through wet deposition. We

371   propose a conceptual model to show the aerosol-cloud interactions on mountaintops influenced by

372   heavily polluted air.

373

374   **Data availability.** All data presented in this paper are available upon request. Please contact the

375   corresponding author (liweijun_atmos@gmail.com).

376

377   **Competing interests.** The authors declare that they have no conflict of interest.

378

References

384   Ackerman, A. S., Toon, O. B., Stevens, D. E., Heymsfield, A. J., Ramanathan, V., and Welton, E. J.:

385   Reduction of tropical cloudiness by soot, Science, 288, 1042-1047, 10.1126/science.288.5468.1042,

386   2000.

387   Adachi, K., Chung, S. H., and Buseck, P. R.: Shapes of soot aerosol particles and implications for their

388   effects on climate, J. Geophys. Res.-Atmos., 115, D15206, 10.1029/2009JD012868, 2010.

389   Chen, H., Laskin, A., Baltrusaitis, J., Gorski, C. A., Scherer, M. M., and Grassian, V. H.: Coal Fly Ash

390   as a Source of Iron in Atmospheric Dust, Environ. Sci. Technol., 46, 2112-2120, 10.1021/es204102f,

391   2012.

392   Cherian, R., Quaas, J., Salzmann, M., and Tomassini, L.: Black carbon indirect radiative effects in a

393   climate model, Tellus Ser. B-Chem. Phys. Meteorol., 69, 10.1080/16000889.2017.1369342, 2017.

394   Draxler, R. R., and Rolph, G. D.: HYSPLIT (HYbrid Single-Particle Lagrangian Integrated Trajectory)

395   Model access via NOAA ARL READY Website, http://ready.arl.noaa.gov/HYSPLIT.php, NOAA Air

396   Resources Laboratory, Silver Spring, MD, 2003.

397   Drewnick, F., Schneider, J., Hings, S. S., Hock, N., Noone, K., Targino, A., Weimer, S., and Borrmann,

398   S.: Measurement of ambient, interstitial, and residual aerosol particles on a mountaintop site in central

399   Sweden using an aerosol mass spectrometer and a CVI, J. Atmos. Chem., 56, 1-20,

400   10.1007/s10874-006-9036-8, 2007.

401   Dusek, U., Frank, G., Hildebrandt, L., Curtius, J., Schneider, J., Walter, S., Chand, D., Drewnick, F.,

402   Hings, S., and Jung, D.: Size matters more than chemistry for cloud-nucleating ability of aerosol

403   particles, Science, 312, 1375-1378, 10.1126/science.1125261, 2006.

404   Ebert, M., Weigel, R., Kandler, K., Günther, G., Molleker, S., Grooß, J. U., Vogel, B., Weinbruch, S.,

405   and Borrmann, S.: Chemical analysis of refractory stratospheric aerosol particles collected within the

406   arctic vortex and inside polar stratospheric clouds, Atmos. Chem. Phys., 16, 8405-8421,

407   10.5194/acp-16-8405-2016, 2016.

408   Eck, T. F., Holben, B. N., Reid, J. S., Xian, P., Giles, D. M., Sinyuk, A., Smirnov, A., Schafer, J. S.,

409   Slutsker, I., Kim, J., Koo, J. H., Choi, M., Kim, K. C., Sano, I., Arola, A., Sayer, A. M., Levy, R. C.,

410   Munchak, L. A., O'Neill, N. T., Lyapustin, A., Hsu, N. C., Randles, C. A., Da Silva, A. M., Buchard, V.,

411   Govindaraju, R. C., Hyer, E., Crawford, J. H., Wang, P., and Xia, X.: Observations of the Interaction

412   and Transport of Fine Mode Aerosols With Cloud and/or Fog in Northeast Asia from Aerosol Robotic

413   Network (AERONET) and Satellite Remote Sensing, J. Geophys. Res.-Atmos., 123, 5560-5587,

414   10.1029/2018JD028313, 2018.

415   Ervens, B.: Modeling the Processing of Aerosol and Trace Gases in Clouds and Fogs, Chem. Rev., 115,

416   4157-4198, 10.1021/cr5005887, 2015.

417   Fan, J., Wang, Y., Rosenfeld, D., and Liu, X.: Review of Aerosol-Cloud Interactions: Mechanisms,

418   Significance, and Challenges, J. Atmos. Sci., 73, 4221-4252, 10.1175/jas-d-16-0037.1, 2016.

419   Farmer, D. K., Cappa, C. D., and Kreidenweis, S. M.: Atmospheric Processes and Their Controlling

420   Influence on Cloud Condensation Nuclei Activity, Chem. Rev., 115, 4199-4217, 10.1021/cr5006292,

421   2015.

422   Fomba, K. W., van Pinxteren, D., Muller, K., Iinuma, Y., Lee, T., Collett, J. L., and Herrmann, H.: Trace

423   metal characterization of aerosol particles and cloud water during HCCT 2010, Atmos. Chem. Phys., 15,

424   8751-8765, 10.5194/acp-15-8751-2015, 2015.

425   Hao, L., Romakkaniemi, S., Kortelainen, A., Jaatinen, A., Portin, H., Miettinen, P., Komppula, M.,

426   Leskinen, A., Virtanen, A., Smith, J. N., Sueper, D., Worsnop, D. R., Lehtinen, K. E. J., and Laaksonen,

427   A.: Aerosol Chemical Composition in Cloud Events by High Resolution Time-of-Flight Aerosol Mass

428   Spectrometry, Environ. Sci. Technol., 47, 2645-2653, 10.1021/es302889w, 2013.

429   Harris, E., Sinha, B., van Pinxteren, D., Tilgner, A., Fomba, K. W., Schneider, J., Roth, A., Gnauk, T.,

430   Fahlbusch, B., and Mertes, S.: Enhanced role of transition metal ion catalysis during in-cloud oxidation

431   of SO_2, Science, 340, 727-730, 10.1126/science.1230911, 2013.

432   Hiranuma, N., Brooks, S. D., Moffet, R. C., Glen, A., Laskin, A., Gilles, M. K., Liu, P., Macdonald, A.

433   M., Strapp, J. W., and McFarquhar, G. M.: Chemical characterization of individual particles and

434   residuals of cloud droplets and ice crystals collected on board research aircraft in the ISDAC 2008 study,

435   J. Geophys. Res.-Atmos., 118, 6564-6579, 10.1002/jgrd.50484, 2013.

436   Hopkins, R. J., Desyaterik, Y., Tivanski, A. V., Zaveri, R. A., Berkowitz, C. M., Tyliszczak, T., Gilles, M.

437   K., and Laskin, A.: Chemical speciation of sulfur in marine cloud droplets and particles: Analysis of

438   individual particles from the marine boundary layer over the California current, J. Geophys.

439   Res.-Atmos., 113, D04209, 10.1029/2007jd008954, 2008.

440   Hudson, J. G.: Variability of the relationship between particle size and cloud-nucleating ability,

441   Geophys. Res. Lett., 34, L08801, 10.1029/2006gl028850, 2007.

442   Ito, A., and Shi, Z.: Delivery of anthropogenic bioavailable iron from mineral dust and combustion

443   aerosols to the ocean, Atmos. Chem. Phys., 16, 85-99, 10.5194/acp-16-85-2016, 2016.

444   Kojima, T., Buseck, P. R., Wilson, J. C., Reeves, J. M., and Mahoney, M. J.: Aerosol particles from

445   tropical convective systems: Cloud tops and cirrus anvils, J. Geophys. Res.-Atmos., 109, D12201,

446   10.1029/2003JD004504, 2004.

447   Li, J., Wang, X., Chen, J., Zhu, C., Li, W., Li, C., Liu, L., Xu, C., Wen, L., Xue, L., Wang, W., Ding, A.,

448   and Herrmann, H.: Chemical composition and droplet size distribution of cloud at the summit of Mount

449   Tai, China, Atmos. Chem. Phys., 17, 9885-9896, 10.5194/acp-17-9885-2017, 2017a.

450   Li, W., Li, P., Sun, G., Zhou, S., Yuan, Q., and Wang, W.: Cloud residues and interstitial aerosols from

451   non-precipitating clouds over an industrial and urban area in northern China, Atmos. Environ., 45,

452   2488-2495, 10.1016/j.atmosenv.2011.02.044, 2011a.

453   Li, W., Zhang, D., Shao, L., Zhou, S., and Wang, W.: Individual particle analysis of aerosols collected

454   under haze and non-haze conditions at a high-elevation mountain site in the North China plain, Atmos.

455   Chem. Phys., 11, 11733-11744, 10.5194/acp-11-11733-2011, 2011b.

456   Li, W., Wang, Y., Collett, J. L., Chen, J., Zhang, X., Wang, Z., and Wang, W.: Microscopic Evaluation of

457   Trace Metals in Cloud Droplets in an Acid Precipitation Region, Environ. Sci. Technol., 47, 4172-4180,

458   10.1021/es304779t, 2013.

459   Li, W., Shao, L., Zhang, D., Ro, C.-U., Hu, M., Bi, X., Geng, H., Matsuki, A., Niu, H., and Chen, J.: A

460   review of single aerosol particle studies in the atmosphere of East Asia: morphology, mixing state,

461   source, and heterogeneous reactions, J. Clean Prod., 112, 1330-1349, 10.1016/j.jclepro.2015.04.050,

462   2016a.

463   Li, W., Sun, J., Xu, L., Shi, Z., Riemer, N., Sun, Y., Fu, P., Zhang, J., Lin, Y., and Wang, X.: A

464   conceptual framework for mixing structures in individual aerosol particles, J. Geophys. Res.-Atmos.,

465   121, 13784-13798, 10.1002/2016JD025252, 2016b.

466   Li, W., Xu, L., Liu, X., Zhang, J., Lin, Y., Yao, X., Gao, H., Zhang, D., Chen, J., and Wang, W.: Air

467   pollution–aerosol interactions produce more bioavailable iron for ocean ecosystems, Sci. Adv., 3,

468   e1601749, 10.1126/sciadv.1601749, 2017b.

469   Lin, Q., Zhang, G., Peng, L., Bi, X., Wang, X., Brechtel, F. J., Li, M., Chen, D., Peng, P., Sheng, G., and

470   Zhou, Z.: In situ chemical composition measurement of individual cloud residue particles at a mountain

471   site, southern China, Atmos. Chem. Phys., 17, 8473-8488, 10.5194/acp-17-8473-2017, 2017.

472   Liu, L., Kong, S., Zhang, Y., Wang, Y., Xu, L., Yan, Q., Lingaswamy, A. P., Shi, Z., Lv, S., Niu, H., Shao,

473   L., Hu, M., Zhang, D., Chen, J., Zhang, X., and Li, W.: Morphology, composition, and mixing state of

474   primary particles from combustion sources — crop residue, wood, and solid waste, Sci. Rep., 7, 5047,

475   10.1038/s41598-017-05357-2, 2017.

476   Liu, X., Wai, K. M., Wang, Y., Zhou, J., Li, P., Guo, J., Xu, P., and Wang, W.: Evaluation of trace

477   elements contamination in cloud/fog water at an elevated mountain site in Northern China,

478   Chemosphere, 88, 531-541, 10.1016/j.chemosphere.2012.02.015, 2012.

479   McFiggans, G., Artaxo, P., Baltensperger, U., Coe, H., Facchini, M. C., Feingold, G., Fuzzi, S., Gysel,

480   M., Laaksonen, A., Lohmann, U., Mentel, T. F., Murphy, D. M., O'Dowd, C. D., Snider, J. R., and

481   Weingartner, E.: The effect of physical and chemical aerosol properties on warm cloud droplet

482   activation, Atmos. Chem. Phys., 6, 2593-2649, 10.5194/acp-6-2593-2006, 2006.

483   Moffet, R. C., Desyaterik, Y., Hopkins, R. J., Tivanski, A. V., Gilles, M. K., Wang, Y., Shutthanandan, V.,

484   Molina, L. T., Abraham, R. G., Johnson, K. S., Mugica, V., Molina, M. J., Laskin, A., and Prather, K. A.:

485   Characterization of Aerosols Containing Zn, Pb, and Cl from an Industrial Region of Mexico City,

486   Environ. Sci. Technol., 42, 7091-7097, 10.1021/es7030483, 2008.

487   Pierce, J., Croft, B., Kodros, J., D'Andrea, S., and Martin, R.: The importance of interstitial particle

488   scavenging by cloud droplets in shaping the remote aerosol size distribution and global aerosol-climate

489   effects, Atmos. Chem. Phys., 15, 6147-6158, 10.5194/acp-15-6147-2015, 2015.

490   Pratt, K. A., Twohy, C. H., Murphy, S. M., Moffet, R. C., Heymsfield, A. J., Gaston, C. J., DeMott, P. J.,

491   Field, P. R., Henn, T. R., Rogers, D. C., Gilles, M. K., Seinfeld, J. H., and Prather, K. A.: Observation of

492   playa salts as nuclei in orographic wave clouds, J. Geophys. Res.-Atmos., 115, D15301,

493   10.1029/2009jd013606, 2010.

494   Qi, J., Zheng, B., Li, M., Yu, F., Chen, C., Liu, F., Zhou, X., Yuan, J., Zhang, Q., and He, K.: A

495   high-resolution air pollutants emission inventory in 2013 for the Beijing-Tianjin-Hebei region, China,

496   Atmos. Environ., 170, 156-168, 10.1016/j.atmosenv.2017.09.039, 2017.

497   Qian, Y., Gong, D., Fan, J., Leung, L. R., Bennartz, R., Chen, D., and Wang, W.: Heavy pollution

498   suppresses light rain in China: Observations and modeling, J. Geophys. Res.-Atmos., 114, D00K02,

499   10.1029/2008JD011575, 2009.

500   Roberts, J. R., Taylor, M. D., Castranova, V., Clarke, R. W., and Antonini, J. M.: Soluble metals

501   associated with residual oil fly ash increase morbidity and lung injury after bacterial infection in rats, J.

502   Toxicol. Env. Health Part A, 67, 251-263, 10.1080/15287390490266927, 2004.

503   Rosenfeld, D.: Suppression of rain and snow by urban and industrial air pollution, Science, 287,

504   1793-1796, 10.1126/science.287.5459.1793, 2000.

505   Rosenfeld, D., Sherwood, S., Wood, R., and Donner, L.: Climate effects of aerosol-cloud interactions,

506   Science, 343, 379-380, 10.1126/science.1247490, 2014.

507   Roth, A., Schneider, J., Klimach, T., Mertes, S., van Pinxteren, D., Herrmann, H., and Borrmann, S.:

508   Aerosol properties, source identification, and cloud processing in orographic clouds measured by single

509   particle mass spectrometry on a central European mountain site during HCCT-2010, Atmos. Chem.

510   Phys., 16, 505-524, 10.5194/acp-16-505-2016, 2016.

511   Schneider, J., Mertes, S., Pinxteren, D. v., Herrmann, H., and Borrmann, S.: Uptake of nitric acid,

512   ammonia, and organics in orographic clouds: mass spectrometric analyses of droplet residual and

513   interstitial aerosol particles, Atmos. Chem. Phys., 17, 1571-1593, 10.5194/acp-17-1571-2017, 2017.

514   Schroder, J., Hanna, S., Modini, R., Corrigan, A., Kreidenweis, S., Macdonald, A., Noone, K. J., Russell,

515   L., Leaitch, W., and Bertram, A.: Size-resolved observations of refractory black carbon particles in

516   cloud droplets at a marine boundary layer site, Atmos. Chem. Phys., 15, 1367-1383,

517   10.5194/acp-15-1367-2015, 2015.

518   Seinfeld, J. H., and Pandis, S. N.: Atmospheric chemistry and physics: from air pollution to climate

519   change, John Wiley & Sons, 2006.

520   Seinfeld, J. H., Bretherton, C., Carslaw, K. S., Coe, H., DeMott, P. J., Dunlea, E. J., Feingold, G., Ghan,

521   S., Guenther, A. B., and Kahn, R.: Improving our fundamental understanding of the role of

522   aerosol−cloud interactions in the climate system, Proc. Natl. Acad. Sci., 113, 5781-5790,

523   10.1073/pnas.1514043113, 2016.

524   Shen, X. H., Lee, T., Guo, J., Wang, X., Li, P., Xu, P., Wang, Y., Ren, Y., Wang, W., Wang, T., Li, Y.,

525   Cam, S. A., and Collett, J. L., Jr.: Aqueous phase sulfate production in clouds in eastern China, Atmos.

526   Environ., 62, 502-511, 10.1016/j.atmosenv.2012.07.079, 2012.

527   Tilgner, A., Schöne, L., Bräuer, P., Van Pinxteren, D., Hoffmann, E., Spindler, G., Styler, S., Mertes, S.,

528   Birmili, W., and Otto, R.: Comprehensive assessment of meteorological conditions and airflow

529   connectivity during HCCT-2010, Atmos. Chem. Phys., 14, 9105-9128, 10.5194/acp-14-9105-2014,

530   2014.

531   Twohy, C. H., and Anderson, J. R.: Droplet nuclei in non-precipitating clouds: composition and size

Atmospheric
Chemistry
and Physics
Discussions

532   matter, Environ. Res. Lett., 3, 10.1088/1748-9326/3/4/045002, 2008.

533   Ueda, S., Hirose, Y., Miura, K., and Okochi, H.: Individual aerosol particles in and below clouds along a

534   Mt. Fuji slope: Modification of sea-salt-containing particles by in-cloud processing, Atmos. Res., 137,

535   216-227, 10.1016/j.atmosres.2013.10.011, 2014.

536   Wang, J., Cubison, M. J., Aiken, A. C., Jimenez, J. L., and Collins, D. R.: The importance of aerosol

537   mixing state and size-resolved composition on CCN concentration and the variation of the importance

538   with atmospheric aging of aerosols, Atmos. Chem. Phys., 10, 7267-7283, 10.5194/acp-10-7267-2010,

539   2010.

540   Wang, Y., Guo, J., Wang, T., Ding, A., Gao, J., Zhou, Y., Collett, J. L., and Wang, W.: Influence of

541   regional pollution and sandstorms on the chemical composition of cloud/fog at the summit of Mt.

542   Taishan in northern China, Atmos. Res., 99, 434-442, 10.1016/j.atmosres.2010.11.010, 2011.

543   Wang, Z., Zhang, H., Li, J., Jing, X., and Lu, P.: Radiative forcing and climate response due to the

544   presence of black carbon in cloud droplets, J. Geophys. Res.-Atmos., 118, 3662-3675,

545   10.1002/jgrd.50312, 2013.

546   Zhang, D., Ishizaka, Y., and Aryal, D.: Individual particles and droplets in continentally influenced

547   stratocumulus: A case study over the Sea of Japan, Atmos. Res., 79, 30-51,

548   10.1016/j.atmosres.2005.04.003, 2006.

549   Zhang, G., Lin, Q., Peng, L., Bi, X., Chen, D., Li, M., Li, L., Brechtel, F. J., Chen, J., Yan, W., Wang, X.,

550   Peng, P., amp, apos, an, Sheng, G., and Zhou, Z.: The single-particle mixing state and cloud scavenging

551   of black carbon: a case study at a high-altitude mountain site in southern China, Atmos. Chem. Phys.,

552   17, 14975-14985, 10.5194/acp-17-14975-2017, 2017.

553   Zhang, Y., Zhang, X., Sun, J., Hu, G. Y., Shen, X., Wang, Y., Wang, T. T., Wang, D. Z., and Zhao, Y.:

554   Chemical composition and mass size distribution of PM1 at an elevated site in central east China,

555   Atmos. Chem. Phys., 14, 12237-12249, 10.5194/acp-14-12237-2014, 2014.

556   Zhao, C., Tie, X. X., and Lin, Y. P.: A possible positive feedback of reduction of precipitation and

557   increase in aerosols over eastern central China, Geophys. Res. Lett., 33, L11814,

558   10.1029/2006gl025959, 2006.

559   Zuberi, B., Johnson, K. S., Aleks, G. K., Molina, L. T., and Laskin, A.: Hydrophilic properties of aged

560   soot, Geophys. Res. Lett., 32, L01807, 10.1029/2004gl021496, 2005.

561